Determination of the W8 and AB5 defect levels in the diamond gap

2001 J. Phys.: Condens. Matter 13 8957

(http://iopscience.iop.org/0953-8984/13/40/311)

INSTITUTE OF PHYSICS PUBLISHING JOURNAL OF PHYSICS: CONDENSED MATTER

J. Phys.: Condens. Matter **13** (2001) 8957–8964 PII: S0953-8984(01)24496-8

Determination of the W8 and AB5 defect levels in the diamond gap

R N Pereira[1,2], W Gehlhoff[2], N A Sobolev[1], A J Neves[1] and D Bimberg[2]

[1] Department of Physics, University of Aveiro, 3810-193 Aveiro, Portugal
[2] Institute of Solid State Physics, TU Berlin, D-10623 Berlin, Germany

E-mail: rui.pereira@fis.ua.pt

Received 3 May 2001
Published 20 September 2001
Online at stacks.iop.org/JPhysCM/13/8957

Abstract

Electron paramagnetic resonance (EPR) and photo-EPR investigations on synthetic diamond crystals have allowed an unambiguous determination of nickel-related defect levels in the diamond bandgap. Indirect photoinduced recharging of the nitrogen donor and detection of two complementary photoionization transitions involving the substitutional nickel show that the $Ni_s^{-/0}$ acceptor state is located at 2.49 ± 0.03 eV below the conduction band. A strong decrease of the AB5 EPR signal intensity is induced by irradiation of the samples with photon energies $h\nu > 1.88$ eV. Observation of a recharging process upon photoexcitation with $h\nu > 2.5$ eV yields the localization of the AB5 defect level position at $E = E_C - 1.88 \pm 0.03$ eV.

1. Introduction

The unique physical properties of diamond and recent advances in its synthesis make diamond an attractive material for numerous applications, from electronic to mechanical purposes. Since, however, these properties are very sensitive to the presence of impurities and defects in the material, the successful exploitation of diamond demands a thorough understanding of the formation and properties of these defects. Nitrogen is the most common impurity found in natural and synthetic diamond, either isolated or forming pairs or small clusters. In synthetic as-grown diamonds the dispersed substitutional nitrogen in the neutral charge state (N_s^0) is typically the most abundant defect. It gives rise to the well established electron paramagnetic resonance (EPR) spectrum labelled P1. Due to the use of transition metals like Ni, Co and Fe as solvents/catalysts in the synthesis of diamond at high pressures and high temperatures (HPHT) it is very likely that these elements are incorporated into the crystal. By the observation of the hyperfine structure of cobalt (^{59}Co, $I = 7/2$, natural abundance 100%) and of nickel enriched with ^{61}Ni ($I = 3/2$, natural abundance 1.2%), EPR studies have directly proven the incorporation of isolated nickel [1] and of cobalt, probably as the CoN complex [2]. Other works have borne strong evidence of the formation of several nickel-related

paramagnetic centres in both synthetic and natural diamonds [3–8]. Although considerable effort has been aimed at searching for optical analogues of some of these defects, up to now little information has been achieved regarding their energy levels in the diamond bandgap. Only for the substitutional Ni_s^- (W8 centre [9]) has an ionization energy of 2.5 eV been determined from EPR measurements upon photoexcitation (photo-EPR). It was suggested that this level is located at 3.0 eV above the valence band [10].

The advantage of the photo-EPR as compared to other methods of the determination of the energy levels of a centre is based upon the fact that it also gathers information concerning the spin state, the symmetry of the defect and, very often, also its chemical nature. Additionally, this technique may provide information about the recombination and trapping of charge carriers.

In the present paper we report the first photo-EPR investigations on the AB5 [4] nickel-related centre together with new photo-EPR results on the W8 and the P1 centres in diamond.

2. Experimental details

We used a set of single crystal diamonds synthesized at the National Institute for Research in Inorganic Materials (NIRIM), Japan. The samples were grown by the temperature gradient method at temperatures in the range 1400–1500 °C using Ni (or Ni–Fe) as solvent/catalyst. Two of the diamond samples were annealed for 4 h at 1600 °C under a stabilizing pressure of 6 GPa. The samples were oriented either by growth facets or by faces polished along the main crystallographic directions.

EPR and photo-EPR measurements were carried out using a Bruker ESP 300E spectrometer mounted with a Q-band ($f \approx 34$ GHz) microwave bridge and a cylindrical TE_{011} cavity at temperatures in the range 4.2–100 K. In order to reduce unintentional infrared irradiation of the samples, we used an Oxford Instruments helium bath cryostat. The samples were always cooled down in the dark to guarantee a thermal equilibrium state prior to the illumination procedure. In the photo-EPR measurements, the samples were irradiated with monochromatic light via a 0.4 mm optical fibre, inserted into the helium cryostat. Light from a 100 W Xe lamp was dispersed by a grating monochromator and coupled into another 0.4 mm optical fibre, at the end of which the spectral dependence of the photon flux was measured. When illuminating the samples, the two fibres were connected.

3. Experimental results and discussion

A major scope of photo-EPR experiments is the determination of the ionization energy of localized states, which can be obtained from the spectral dependence of the optical cross section. The requirements for a correct determination of this dependence from the photo-EPR data were extensively discussed by Godlewski [11]. The applicability of a definite method is essentially determined by the time dependence of the involved processes. In the temperature range of our measurements, the photoinduced changes of the defect level population were metastable and it was difficult to ensure the same starting population for the centre under study prior to each subsequent photoexcitation. Therefore, we used the saturation method, which is based on the determination of the difference ΔI_{EPR} between the EPR signal intensity I_{EPR} measured prior to illumination with a certain wavelength and its photoinduced saturation value [11] and allows, in a simple way, the consideration of different starting populations. With the external magnetic field being fixed at the position of maximum intensity of the first derivative of the corresponding EPR line, we measured the time dependence of I_{EPR} upon an illumination sequence with

increasing photon energies, see figure 1. The spectral dependence of ΔI_{EPR} for the centre under study was then estimated through fitting the data by exponential decay functions.

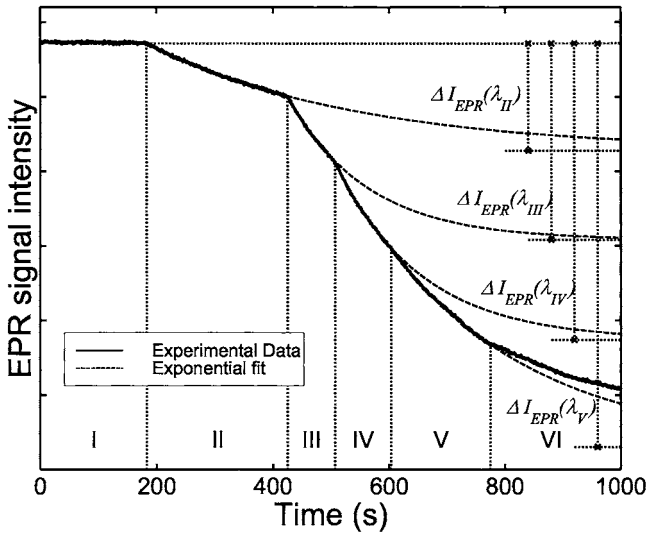

Figure 1. Time dependence of the EPR signal intensity I_{EPR} of the AB5 centre at $T = 60$ K for different excitation photon energies $h\nu$ (eV) = 1.87 (I), 1.96 (II), 2.06 (III), 2.15 (IV), 2.23 (V), 2.32 (VI). Full curves represent experimental data and dashed curves are exponential fits. Horizontal lines represent the saturation values obtained from the fits. One exponential cannot fit the data in the interval VI because another photoionization process sets in at this energy [13]. The vertical bars represent the ΔI_{EPR} values used for the determination of the optical cross sections.

3.1. W8 and P1 centres: photo-EPR

For the measurements of the dependence of the W8 EPR signal intensity on the photoexcitation wavelength, diamond samples exhibiting only two spectra, a strong W8 and a weak P1, were chosen. The dependence of ΔI_{EPR} of W8 on the photoexcitation energy normalized to a constant photon flux is shown in figure 2(a). The EPR signal intensity starts to decrease exponentially at a photon energy threshold of 2.5 eV, in agreement with [10]. A complete description of the ΔI_{EPR} dependence on the optical cross section for a photoionization transition (PT) requires the solution of a complex system of kinetic equations that would consider all excitation, recombination and capture processes occurring at the levels involved. In practice, different approaches are used to simplify the kinetic equations and facilitate their solution. The time dependence of the population of the W8 centre, neglecting carrier recombination and thermal emission, can be described by the equation

$$\frac{\mathrm{d}N_{W8}}{\mathrm{d}t} = I\sigma_h^{Ni}(N_{Ni} - N_{W8}) - I\sigma_e^{Ni}N_{W8} + C_e^{Ni}n(N_{Ni} - N_{W8}) - C_h^{Ni}pN_{W8} \tag{1}$$

where N_{Ni} is the total amount of substitutional nickel and N_{W8} is the number of Ni atoms in the paramagnetic state (Ni_s^-). σ_e^{Ni} and σ_h^{Ni} are the cross sections of the two complementary photoinduced transitions involving the nickel level, i.e. electron promotion from the impurity level to the conduction band (CB) and hole ionization from the impurity level to the valence band (VB), respectively. C_e^{Ni} and C_h^{Ni} are capture rates of electrons and holes by the impurity. I is the photon flux; n and p are the numbers of free electrons and holes, respectively. As

pointed out above, the W8 EPR signal intensity remains nearly constant after the light is turned off. This indicates a low efficiency of the recombination processes and also indicates that free carriers excited to the CB from the nickel level are also being trapped by other deep centres not considered in equation (1). The analysis of the photoinduced processes can be simplified when only the defect level under study is ionized by the incident light and when, moreover, the photon energy induces transitions between the defect level and only one of the allowed energy bands. This holds true for the W8 photoinduced transition at 2.5 eV, taking into account that this is the dominant process and that only one of the two complementary PTs can be active in the 5.5 eV wide diamond bandgap for $h\nu < 3$ eV. In such a case the overall kinetic process depends on the light intensity only through one of the $\alpha_i = I \times \sigma_i$ $(i = e, h)$ values, and ΔI_{EPR} has the same dependence on I and the particular σ_i. The change of ΔI_{EPR} versus α, in the case of photoinduced quenching of W8 with $h\nu = 2.72$ eV, is shown in figure 3. ΔI_{EPR} varies linearly with α for low light intensity and saturates for higher intensities. *Vice versa*, for a given photon flux I, the saturation is more easily achieved for higher $h\nu$ values, i.e. larger cross sections σ. In the linear regime, ΔI_{EPR} is directly proportional to the corresponding optical cross section. The data points presented in figure 2 were obtained under this experimental condition. Fitting the spectral dependence $\sigma(h\nu)$ of the W8 excitation by the Lucovsky formula for a purely electronic cross section [12]

$$\sigma(E_t, h\nu) \propto \frac{(h\nu - E_t)^{3/2}}{(h\nu)^3} \tag{2}$$

we found the ionization energy $E_t = 2.49 \pm 0.03$ eV for the W8 centre, see figure 2(a). In order to clarify the nature of the process that causes the changes of the W8 signal intensity we suppressed the latter to its lowest value by applying a high-intensity photoexcitation with $h\nu \approx 2.7$ eV and then tracked the recovery of the EPR signal intensity upon illumination of the sample with $h\nu > 2.7$ eV. A threshold energy for which the W8 EPR signal intensity starts to increase exponentially was found, see figure 2(b). The best fit of the experimental data by equation (2) is obtained for $E_t = 3.00 \pm 0.05$ eV. As this value added to the previously measured 2.5 eV photoionization threshold matches the 5.5 eV wide bandgap of diamond, we conclude that this process is the complementary photoionization transition occurring at the $Ni^{-/0}$ level and that the lattice stabilization energy [11] is very small. The observation of the two complementary photoionization transitions indicates that the photoinduced changes of the W8 EPR signal intensity result mainly from the direct photoionization of the W8 centre.

To find out whether the 2.5 eV ionization process observed for the W8 centre involves the promotion of electrons to the CB or that of holes to the VB, we monitored the photoinduced changes of the EPR signal intensity of the N_S^0 deep donor (P1 centre), proceeding in a similar way to that described above for the W8 centre. Figure 2(c) shows the spectral dependence of the photoinduced enhancement of the P1 EPR signal. The signal intensity starts to increase gradually at photon energies $h\nu > 2.5$ eV. An indirect process can explain this increase: the illumination induces the photoionization of the W8 centre and the electrons promoted to the CB are then captured by the nitrogen. In order to exclude the possibility that the photoelectrons are generated from a centre other than Ni, the recharging process of the P1 centre was investigated in detail. Under the experimental conditions described above, the ΔI_{EPR} values of P1 are proportional to the optical cross section of the involved level. Fitting the data in figure 2(c) by equation (2), we obtain the threshold energy $E_t = 2.45 \pm 0.05$ eV that is in good agreement with the 2.49 eV ionization energy found from the direct ionization process of the W8 centre. The observation of this indirect recharging of the nitrogen deep donor permits an unambiguous localization of the $Ni_S^{-/0}$ acceptor level at 2.49 eV below the conduction band.

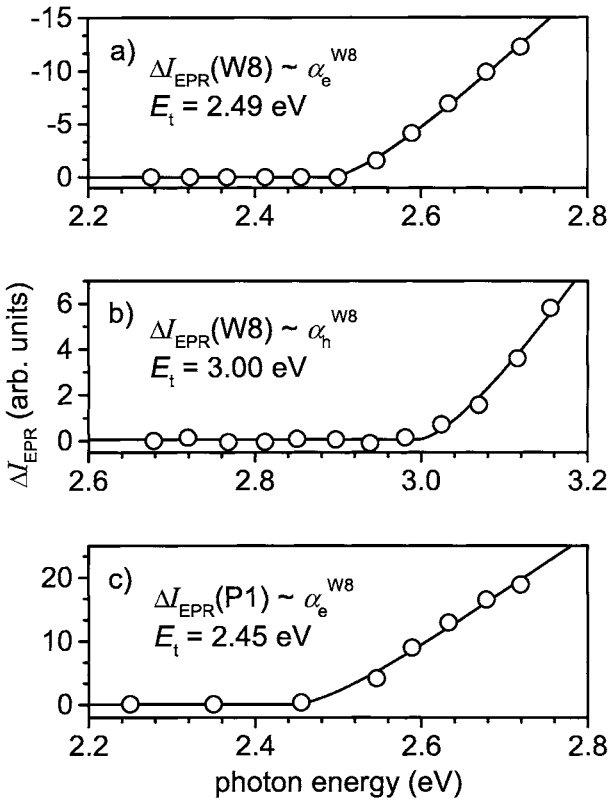

Figure 2. (a) Dependence of the quenching of the EPR signal (ΔI_{EPR} as defined in figure 1) versus the photon energy for the W8 centre. (b) Spectral dependence of the recovery of the W8 EPR signal previously quenched by illumination with $h\nu = 2.72$ eV. In this case, ΔI_{EPR} is measured relative to the minimum signal intensity achieved after a prolonged illumination. (c) Spectral dependence of the enhancement of the P1 EPR signal. The circles represent experimental values and the full curves are fits to the data by the Lucovsky formula, equation (2).

3.2. AB5 centre

The AB5 centre was detected for the first time in annealed HPHT diamond samples. This trigonal centre has an electron spin $S = 1$ and was tentatively assigned to a nickel–nitrogen pair in the negative charge state [4]. Due to the large zero-field splitting $D = 1.06$ cm^{-1}, the EPR spectrum pattern is strongly dependent on the energy of microwave quanta used; moreover, in both the X- and Q-bands the line positions and line intensities exhibit a strong angular dependence, which hinders the detection of the AB5 lines. Nevertheless, our EPR studies of a set of HPHT synthetic diamonds grown using Ni or Ni–Fe alloys reveal that this centre, along with W8 and P1, is always detectable in as-grown and annealed crystals grown without nitrogen getters. On the other hand, the corresponding EPR signal is absent in samples with low nitrogen content grown with nitrogen getters. These facts suggest that nitrogen is a possible constituent of AB5.

In order to determine the energy level of the AB5 centre in the bandgap, photo-EPR investigations similar to those described above for the W8 centre were done for three diamond crystals that exhibited sufficient signal intensity.

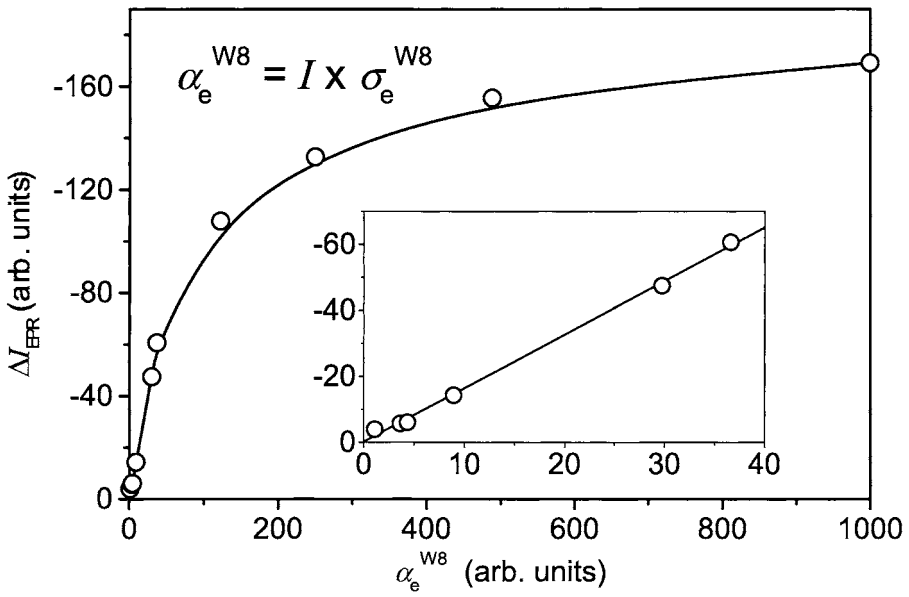

Figure 3. (a) Dependence of the quenching of the W8 EPR signal (ΔI_{EPR} as defined in figure 1) versus $\alpha = I \times \sigma$. The photon energy is fixed at $h\nu = 2.72$ eV and the light intensity is varied. The circles represent experimental values and the full curve is a guide for the eyes only. (b) The same dependence for small α values. The full curve is a linear fit to the data.

The time dependence of the AB5 signal intensity was recorded at $T = 60$ K for different photoexcitation energies, see figure 1, and the ΔI_{EPR} values were determined as before. The spectral dependence of ΔI_{EPR} normalized to a constant photon flux is presented in figure 4(a). There is a photon energy threshold of about 1.9 eV for the observed strong decrease of the signal intensity. This threshold is sample independent. All other centres observed in these samples exhibit photoexcitation processes with different spectral dependences and/or sample-dependent threshold energies [13]. This indicates that the observed AB5 quenching process occurs due to direct photoionization. Although the presence of other defects in the sample may influence the kinetics of the observed depopulation of the AB5 level they do not change its energy threshold, for the latter results from a direct ionization of the AB5 centre. There are only two possible electron transitions, namely, that from the impurity level to the CB or that from the VB to the impurity level, with optical cross sections σ_e^{AB5} and σ_h^{AB5}, respectively. Under the assumption of only one dominant transition and excluding photoionization of other defect levels, the kinetics of the AB5 photoionization can be linked to the light intensity either through $\alpha_e^{AB5} = I \times \sigma_e^{AB5}$ or through $\alpha_h^{AB5} = I \times \sigma_h^{AB5}$. The data shown in figure 4(a) were obtained under the condition of a linear relation between ΔI_{EPR} and the corresponding α^{AB5} value. Fitting the spectral dependence of these experimental data by equation (2), we obtained for the AB5 centre the ionization energy $E_t = 1.88 \pm 0.03$ eV. Since the detected photoquenching can be caused by the electron or hole ionization, the locations of the level below the CB or above the VB are indistinguishable. In order to verify the nature of this transition, we suppressed the AB5 signal intensity by photoexcitation with the photon energy $\approx$2.3 eV to its minimum value and monitored the changes in the signal intensity upon illumination with photon energies $h\nu > 2.3$ eV. We found that the signal intensity increases upon illumination with $h\nu > 2.5$ eV. Fitting, for each photoexcitation, the time dependence of this increase by exponential decay

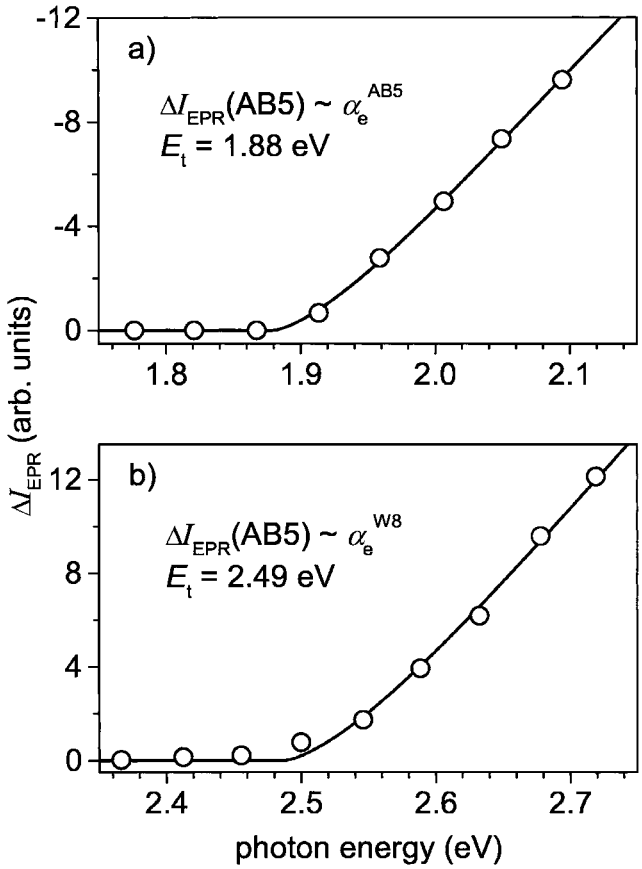

Figure 4. (a) Dependence of the quenching of the EPR signal (ΔI_{EPR} as defined in figure 1) versus the photon energy for the AB5 centre. (b) Spectral dependence of the recovery of the AB5 EPR signal previously quenched by illumination with $h\nu = 2.23$ eV. In this case, ΔI_{EPR} is measured relative to the minimum signal intensity achieved after a prolonged illumination. The circles represent experimental values and the full curves are fits to the data by the Lucovsky formula, equation (2).

functions, we determined the spectral dependence of ΔI_{EPR}, see figure 4(b). The optical cross section σ_e^{Ni} may be considered to be linearly proportional to the ΔI_{EPR} values of the AB5 recharging process. The increase of the AB5 signal intensity can be explained by an indirect process similar to the previously described recharging of nitrogen, i.e. electrons photoexcited from the nickel centre are subsequently captured by the AB5 defect. In general, this process depends on both the optical cross sections σ_e^{Ni} and σ_e^{AB5}. As a matter of fact, the photo-EPR data on the AB5 centre show that the cross section σ_e^{AB5} cannot be neglected. Thus, at energies higher than 2.5 eV we have to consider both transitions, namely from W8 to CB and from AB5 to CB. However, it is evident from the EPR spectra that the concentration of the substitutional nickel in the investigated samples is always much higher than that of the AB5 defects. For this reason, the photoelectrons produced by the illumination with photon energies $h\nu > 2.5$ eV are mainly created through the ionization of the W8 centres. The best fit of the spectral dependence of ΔI_{EPR} by equation (2) is obtained for $E_t = 2.49 \pm 0.04$ eV, in excellent agreement with the value measured from the direct ionization of the $Ni_s^{-/0}$ acceptor level. The observation of

this indirect recharging of AB5 together with the unambiguous localization of the $Ni_S^{-/0}$ level at $E = E_C - 2.49$ eV provide a direct proof that the photoionization process detected on the AB5 centre at 1.88 eV involves the promotion of electrons to the conduction band. Thus, the recharging level of the AB5 defect is located at $E = E_C - 1.88$ eV.

4. Conclusions

In conclusion, we have investigated the photoinduced recharging processes involving the paramagnetic nickel and nitrogen impurities as well as the recently discovered Ni-related AB5 centre with $S = 1$ in diamond. We have unambiguously proven that the $Ni_s^{-/0}$ level is located at $E = E_C - (2.49 \pm 0.03)$ eV and found that the AB5 defect level is situated at $E = E_C - (1.88 \pm 0.03)$ eV.

Acknowledgments

The work was supported in part by the 'Acções Integradas Luso-Alemãs', Project No A-13/99. The authors would like to thank H Kanda (NIRIM, Japan) for supplying the samples. RNP acknowledges the financial support from FCT under contract PRAXIS XXI/BD/18405/98.

References

[1] Samoilovich M I, Bezrukov G N and Butuzov V P 1971 *JETP Lett.* **14** 379
[2] Twitchen D J, Baker J M, Newton M E and Johnston K 2000 *Phys. Rev.* B **61** 9
[3] Nadolinny V A, Yelisseyev A P, Yuryeva O P and Feygelson B N 1997 *Appl. Magn. Reson.* **12** 543
[4] Neves A J, Pereira R, Sobolev N A, Nazaré M H, Gehlhoff W, Naeser A and Kanda H 2000 *Diamond Relat. Mater.* **9** 1057
[5] Neves A J, Pereira R, Sobolev N A, Nazaré M H, Gehlhoff W, Naeser A and Kanda H 1999 *Physica* B **273–274** 651
[6] Isoya J, Kanda H and Uchida Y 1990 *Phys. Rev.* B **42** 9843
[7] Noble C J, Pawlik Th and Spaeth J-M 1998 *J. Phys.: Condens. Matter* **10** 11 781
[8] Pawlik Th, Noble C and Spaeth J-M 1998 *J. Phys.: Condens. Matter* **10** 9833
[9] Isoya J, Kanda H, Norris J R, Tang J and Bowman M R 1990 *Phys. Rev.* B **41** 3905
[10] Hofmann D M, Ludwig M, Christmann P, Volm D, Meyer B K, Pereira L, Santos L and Pereira E 1994 *Phys. Rev.* B **50** 17 618
[11] Godlewski M 1985 *Phys. Status Solidi* a **90** 11
[12] Lucovsky G 1965 *Solid State Commun.* **3** 299
[13] Pereira R N, Gehlhoff W, Sobolev N A, Neves A J and Bimberg D 2001 *21st Int. Conf. on Defects in Semiconductors (ICDS-21)* p 1